Journal of the Ceramic Society of Japan 131 [10] 771-776 2023
DOI https://doi.org/10.2109/jcersj2.23115

JCS-Japan

SPECIAL ARTICLE-ACADEMIC ACHIEVEMENTS

The 77th CerSJ Awards for Academic Achievements in Ceramic Science and Technology: Review

Novel functional properties of charge-transition oxides synthesized under high pressure

Yuichi Shimakawa[1,†]

[1]**Institute for Chemical Research, Kyoto University, Gokasho Uji, Kyoto 611–0011, Japan**

Oxides containing unusually high-valence transition-metal ions often exhibit charge transitions to relieve the electronic instabilities. A-site-ordered quadruple perovskites $LnCu_3Fe_4O_{12}$ with the unusually high-valence $Fe^{3.75+}$, which are synthesized under high-pressure conditions, show intermetallic-charge-transfer transitions. In this review article, novel thermo-related functional properties induced by the charge transitions in $LnCu_3Fe_4O_{12}$ are highlighted. A large negative-thermal-expansion behavior was observed at the intermetallic-charge-transfer transition temperature. The negative-thermal-expansion property is primarily caused by the size effect of constituent ions by the charge changes. The property is useful for developing materials to compensate the normal positive thermal expansion. Significant latent heat was also found to be provided by the intermetallic-charge-transfer transition in $LnCu_3Fe_4O_{12}$. The large latent heat is considered to be related with unusual first-order magnetic entropy change induced by the charge transition. The large entropy change can be utilized for thermal control through a caloric effect, which can make effective energy systems for thermal energy storage and refrigeration.

Key-words : Functional properties, Transition-metal oxides, Charge transitions, Negative-thermal expansion, Caloric effects

[Received June 5, 2023; Accepted July 21, 2023]

1. Introduction

Transition-metal ions in oxides often adopt various valence states. In iron oxides, Fe ions typically show 2+ and 3+ valence states as seen in FeO and Fe_2O_3, respectively. Higher valence states of Fe like Fe^{4+} can also be stabilized in some oxides, which are synthesized under strong oxidizing conditions.[1)–3)] Such unusually high valence states of Fe are intrinsically metastable and often exhibit charge transitions to relieve the electronic instabilities.[4)–7)] Two representative charge transitions of the unusually high-valence Fe ions, i.e., charge-disproportionation and intermetallic-charge-transfer transitions, are known. The charge-disproportionation transition of Fe^{4+} was discovered in 1977,[2)] followed by many related charge-transition phenomena.[8)–12)] Since then the transition behaviors driven by the charge changes have been extensively studied in solid-state chemistry and condensed matter physics research fields for nearly 50 years.

In the charge disproportionation transition of the unusually high valence Fe, a uniform charge state changes to distinct ones. Typical examples are $2Fe^{4+} \rightarrow Fe^{3+} + Fe^{5+}$ found in perovskite structured $CaFeO_3$ and $CaCu_3Fe_4O_{12}$.[2),11)] The metastable Fe^{4+} changes to the stable Fe^{3+} and Fe^{5+}, which are ordered in rock-salt type manner in the perovskite-type crystal structures.[11),13),14)] In the intermetallic-charge-transfer transition, on the other hand, another transition-metal cation involves and changes its valence state as well as the Fe valence state. An example was found in $LaCu_3Fe_4O_{12}$, in which the transition described as $3Cu^{2+} + 4Fe^{3.75+} \rightarrow 3Cu^{3+} + 4Fe^{3+}$ occurs to relieve the instability of the unusually high valence $Fe^{3.75+}$.[12)] Although the ilmenite $FeTiO_3$ and the perovskite $BiNiO_3$ were reported to exhibit the pressure-induced intermetallic-charge-transfer transitions,[15),16)] $LaCu_3Fe_4O_{12}$ was the first example to show the temperature-induced transition at an ambient pressure condition. Because two distinct transition-metal ions are involved and changed the valence states concomitantly with each other, drastic changes in the crystal and electronic structures by the transitions are often observed. Interestingly and importantly, some of the property changes can be utilized as functional properties. In this article, novel thermo-related functional properties, negative-thermal expansion and a caloric effect found in intermetallic-charge-transfer transitions of $LnCu_3Fe_4O_{12}$, are highlighted.

2. Material synthesis

During a solid-state reaction process applying pressure expands area of metastable compounds and increase possibility for discovering new materials. High-pressure synthe-

† Corresponding author: Y. Shimakawa; E-mail: shimak@scl.kyoto-u.ac.jp

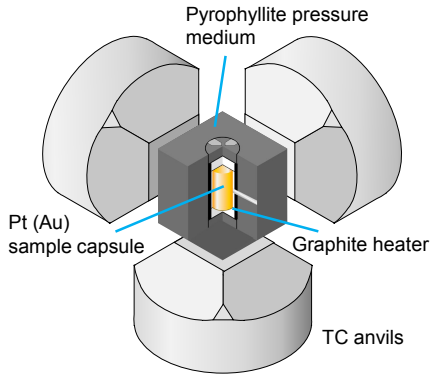

Fig. 1. Schematic picture of a cubic anvil-type high-pressure apparatus. Samples are reacted in a platinum or gold capsule.

sis thus provides access to novel compounds, which cannot be formed with conventional thermodynamic methods, and can be a powerful technique for seeking novel functional materials.[17)]

In synthesizing transition-metal oxides under high pressure, dense crystal structures like the perovskite, which consists of close packing of oxygen and alkaline-earth-metal ions, are often stabilized. Another advantage of the high-pressure synthesis concerns that reaction atmosphere can be tuned within a confined condition. When an oxidizing agent $KClO_4$ is included with raw materials in a sample cell, strong oxidizing conditions can be provided. Perovskite-related structure oxides including cations with the unusually high valence states can often be obtained by the high-pressure synthesis with $KClO_4$.

In the present study we use a cubic anvil-type high-pressure apparatus.[18),19)] The anvils are made of a super-hard sintered tungsten carbide alloy. The six anvils synchronously compress a sample cell through a pyrophyllite medium in a quasi-isostatic pressure condition (**Fig. 1**). Compared to a high-pressure device known as diamond anvil cell, large amount of samples can be easily obtained. Raw oxide materials with $KClO_4$ are packed into a platinum or gold capsule. Heating is achieved using a cylindrical graphite heater and monitored using a thermocouple between the sample capsule and anvil faces. Typical conditions for the synthesis of $LnCu_3Fe_4O_{12}$ are 6–15 GPa and 800–1300 °C for 30 min. After the synthesis reaction the sample is quenched to room temperature followed by releasing pressure. The resultant sample is washed with distilled water to remove the remaining KCl.

3. Crystal structure and intermetallic-charge-transfer transition

$LnCu_3Fe_4O_{12}$ crystalizes in an A-site-ordered quadruple perovskite structure, which is derived from a 1:3 ordered arrangement of the A-site ions in the simple perovskite structure ABO_3. [See the crystal structure in **Fig. 2**(a).][19),20)] By synthesis in a strong oxidizing atmosphere, all oxygen sites are fully occupied, indicating stoichiometric compositions of the compounds. Significant in-phase cooperative octahedral tilting of the corner-sharing BO_6 octahedra

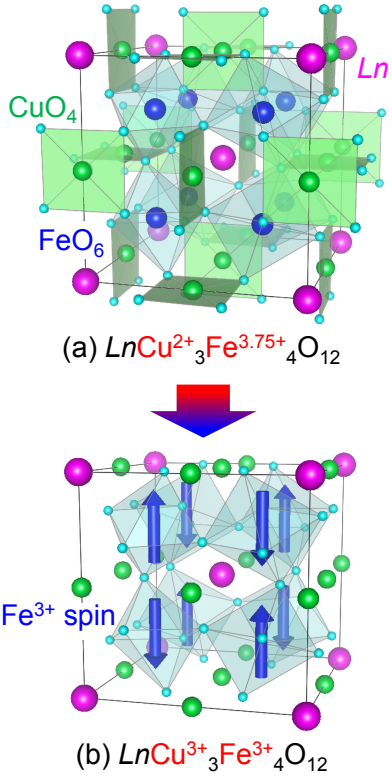

Fig. 2. Crystal and magnetic structures of A-site-ordered quadruple perovskites $LnCu_3Fe_4O_{12}$. The phase changes from (a) the high-temperature $Ln^{3+}Cu^{2+}{}_3Fe^{3.75+}{}_4O_{12}$ to (b) the low-temperature $Ln^{3+}Cu^{3+}{}_3Fe^{3+}{}_4O_{12}$ by the intermetallic-charge-transfer transitions. The Fe^{3+} magnetic moments in the low-temperature $Ln^{3+}Cu^{3+}{}_3Fe^{3+}{}_4O_{12}$ are G-type antiferromagnetically ordered.

($a^+a^+a^+$) makes the $2a \times 2a \times 2a$ unit cell (a represents the unit cell of the ABO_3 simple cubic perovskite structure.), giving Im–3 space group symmetry.[21)–23)] While the A site in $AA'_3B_4O_{12}$ accommodates relatively large cations such as alkaline metal, alkaline-earth metal, or lanthanide, similar to the A site in ABO_3, the A′ site can accept transition-metal ions like Cu, forming square-coordinated units that align perpendicular to each other. Therefore, this structure type oxides include two kinds of valence-variable transition-metal ions at the A′ and B sites, Cu at the A′ site and Fe at the B site in $LnCu_3Fe_4O_{12}$, and the intermetallic charge transfer between them can be induced.

Compounds with Ln = La, Pr, Nd, Sm, Eu, Gd, Tb, and Bi were reported to show the temperature-induced intermetallic-charge-transfer transitions.[24)–26)] The transition is describes as a nominal-ionic-formula change from the high-temperature $Ln^{3+}Cu^{2+}{}_3Fe^{3.75+}{}_4O_{12}$ to the low-temperature $Ln^{3+}Cu^{3+}{}_3Fe^{3+}{}_4O_{12}$. The changes in the valence states of both Cu and Fe respectively at the A′ and B sites ($3Cu^{3+} + 4Fe^{3+} \rightarrow 3Cu^{2+} + 4Fe^{3.75+}$) were confirmed by bond-valence-sum analysis from the refined crystal structures and X-ray absorption and Mössbauer spectroscopy results.[5),12),27)] As shown in the results for $LaCu_3Fe_4O_{12}$ (**Fig. 3**), almost temperature-independent low resistivity increases abruptly below the intermetallic-charge-transfer

transition temperature, suggesting a metal-to-insulator transition. A peak in the temperature-dependent magnetic susceptibility indicates an antiferromagnetic transition accompanied with the intermetallic-charge transfer transition. A G-type antiferromagnetic order, where each Fe^{3+} magnetic moment is antiparallel to the six nearest neighbors, was revealed from the magnetic structure analysis with powder neutron diffraction data. [See also the magnetic structure in Fig. 2(b).][28),29)] This magnetic ordering is ascribed to the B-site Fe^{3+}–O–Fe^{3+} antiferromagnetic superexchange interaction.

The intermetallic-charge-transfer transition temperature of $LnCu_3Fe_4O_{12}$ increases from 233 K (Ln = Tb) to 428 K (Ln = Bi) with increasing the ionic radius of the A-site Ln ion, as shown in **Fig. 4**.[12),24)–26)] The observed nearly linear change suggests that variation in the transition temperature is primarily determined by the size effect of constituent ions in the oxides.

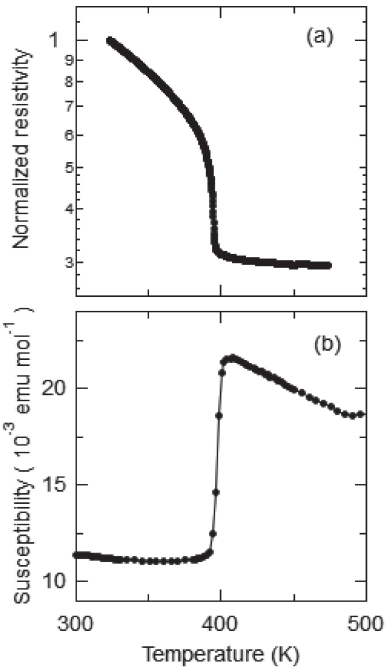

Fig. 3. Temperature dependence of (a) normalized resistivity and (b) magnetic susceptibility of $LaCu_3Fe_4O_{12}$.

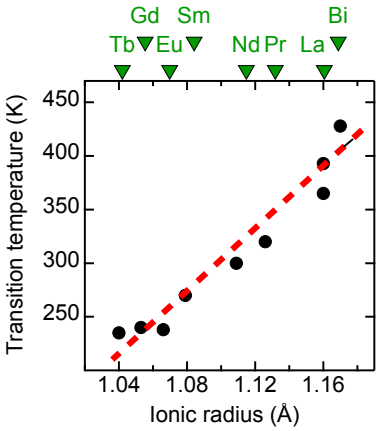

Fig. 4. Intermetallic-charge-transfer transition temperature as a function of ionic radius of the A-site Ln ion in $LnCu_3Fe_4O_{12}$ (Ln = La, Pr, Nd, Sm, Eu, Gd, Tb, or Bi).

4. Negative-thermal expansion

Thermal expansion is a normal behavior of solids upon heating. When a solid material is heated, constituent atoms and molecules vibrate and move to increase the distances between themselves. The thermal expansion in solids often causes problems in many technology fields, and a well-known example is difficulty in precise position control in optical devices under various temperature conditions. It is thus demanded to develop materials with negative thermal expansion properties that can compensate the normal positive thermal expansion.[30)–32)]

When temperature decreases across the intermetallic-charge-transfer transition temperature, $LnCu_3Fe_4O_{12}$ (Ln = La, Pr, Nd, Sm, Eu, Gd, Tb, or Bi) undergoes an isostructural transition and the unit cell volume (a^3) abruptly increases at the transition temperature.[12),24)–26)] In seeing this change in a reverse way, the sample volume of the compound decreases significantly with increasing temperature, and thus the change can be regarded as a negative-thermal-expansion-like behavior. The unit-cell volume change for $LaCu_3Fe_4O_{12}$ with the intermetallic-charge-transfer transition temperatures of 393 K is shown in **Fig. 5**(a), and the negative thermal expansion by ≈1.0 % was observed.[12)]

The observed negative-thermal-expansion-like unit-cell volume change is well explained by a simple ionic-bond model of the program SPuDS.[33),34)] Temperature-dependent unit-cell volumes of $La^{3+}Cu^{2+}{}_3Fe^{3.75+}{}_4O^{2-}{}_{12}$

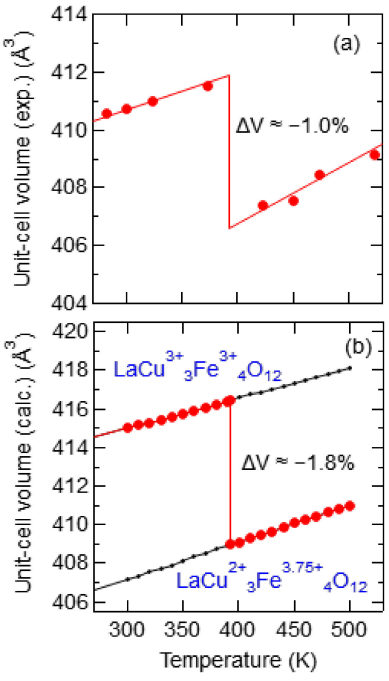

Fig. 5. Temperature dependence of unit-cell volume of $LaCu_3Fe_4O_{12}$ with the intermetallic-charge-transfer transition at 393 K. (a) The unit-cell volumes of experimentally observed and (b) those of $La^{3+}Cu^{2+}{}_3Fe^{3.75+}{}_4O^{2-}{}_{12}$ and $La^{3+}Cu^{3+}{}_3Fe^{3+}{}_4O^{2-}{}_{12}$ calculated with the SPuDS program.

and $La^{3+}Cu^{3+}{}_3Fe^{3+}{}_4O^{2-}{}_{12}$ calculated with the SPuDS program are presented in Fig. 5(b). In the calculation temperature-dependent bond-valence-sum parameters for the constituent cations were used.[35] At a given temperature, the high-temperature $La^{3+}Cu^{2+}{}_3Fe^{3.75+}{}_4O^{2-}{}_{12}$ phase has a smaller unit-cell volume than the low-temperature $La^{3+}Cu^{3+}{}_3Fe^{3+}{}_4O^{2-}{}_{12}$ phase. Provided that the intermetallic-charge-transfer transition between the phases occurs at 393 K, the negative-thermal-expansion-like volume change of about 1.8 % is predicted.[26] The calculated change qualitatively reproduces well the experimentally observed negative-thermal-expansion behavior of $LaCu_3Fe_4O_{12}$. Because the ionic radius of Fe^{4+} with octahedral oxygen coordination (0.585 Å) is smaller than that of Fe^{3+} (0.645 Å),[36] the rigid octahedra get smaller due to decrease in the Fe–O bond lengths, which would drive contraction of the cubic-perovskite unit cell by the intermetallic-charge-transfer transition. An elastic energy term in the intermetallic-charge-transfer transition plays an essential role for the volume change. It is thus concluded that the observed negative-thermal-expansion property is primarily caused by the size effect of constituent ions in the charge-transition oxides.

It is noted, as displayed in Fig. 4, that the intermetallic-charge-transfer transition temperature of $LnCu_3Fe_4O_{12}$ linearly changes by the chemical substitution at the A site. Fine control in the transition temperature with A-site solid-solution compounds can be made.[24–26] Interestingly, the SPuDS calculations predict that the volume difference between the high-temperature $Ln^{3+}Cu^{2+}{}_3Fe^{3.75+}{}_4O^{2-}{}_{12}$ and low-temperature $Ln^{3+}Cu^{3+}{}_3Fe^{3+}{}_4O^{2-}{}_{12}$ phases decreases from 2.9 % (Ln = Tb) to 1.9 % (Ln = La) with increasing the ionic radius of Ln.[26] The trend was experimentally seen and indeed the ≈1.7 % huge negative-thermal-expansion-like change at 310 K was reported in $NdCu_3Fe_4O_{12}$.[25,37] Therefore, precise tuning of the operating temperature and the volume change for the negative-thermal-expansion property becomes possible near room temperature, which is a preferable feature for applications.

5. Caloric effects

Materials showing caloric effects can be used to make effective energy systems for thermal energy storage and refrigeration, and thus have potential for highly efficient and environmentally friendly thermal control applications.[38–42] Typical three ways of controlling thermal properties by the caloric effects are known; magnetocaloric, electrocaloric, and barocaloric effects induced respectively by applying magnetic fields, electric fields, and pressure.[43–47] Development of solid materials that show large caloric effects are of great interest in recent years.

When the intermetallic-charge-transfer transition occurs in $LnCu_3Fe_4O_{12}$, significant latent heat was found to be provided. For $NdCu_3Fe_4O_{12}$ latent heat of 25.5 kJ kg^{-1} on cooling and the corresponding entropy change of 84.2 J K^{-1} kg^{-1} were observed at the intermetallic-charge-transfer-transition temperature near room temperature (**Fig. 6**).[33,48] This entropy change is comparable to the largest entropy change reported in the inorganic $(MnNiSi)_{0.62}(FeCoGe)_{0.38}$ alloy.[49] Importantly, the large latent heat associated with the intermetallic-charge-transfer transition was accessible by applying pressure. The entropy changes $S(T, P)$ as a function of temperature under various pressure is shown in **Fig. 7**(a). As shown in Fig. 7(b), the maximum value of pressure-induced isothermal entropy change ΔS_p was found to reach 65.1 J K^{-1} kg^{-1} at 5.1 kbar and 293.9 K, which correspond to 77 % of the total entropy change associated with the intermetallic-charge-transfer transition under an ambient pressure condition. The pressure-induced adiabatic temperature change reached 13.7 K at the intermetallic-charge-transfer-transition temperature. It was therefore demonstrated that $NdCu_3Fe_4O_{12}$ showed the giant barocaloric effects by the intermetallic-charge-transfer transition.

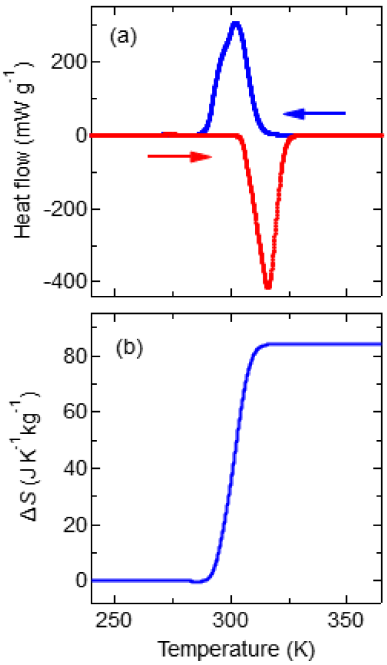

Fig. 6. (a) Heat flow of $NdCu_3Fe_4O_{12}$ measured by differential scanning calorimetry on cooling and heating. (b) Corresponding entropy change ΔS on cooling referred to the value at 360 K.

The giant barocaloric effects with the large entropy changes under pressure are considered to be related with unusual magnetic entropy changes induced by the charge transitions. In $NdCu_3Fe_4O_{12}$ development of the Fe magnetic moment, which was obtained from the neutron magnetic diffraction data, was first order as shown in **Fig. 8**. The behavior is completely different from those observed in normal second-order magnetic transitions induced by usual magnetic interactions between the constituent spins.[33,50,51] The projected magnetic transition temperature extrapolated from the fitting with a Brillouin function to the temperature dependent refined magnetic moment is 643 K, which is much higher than the actual magnetic transition temperature induced by the intermetallic-charge-transfer-transition occurring near room temperature. Given a simple order–disorder magnetic transition model of the $S = 5/2$ (Fe^{3+}) spins, the magnetic entropy change is

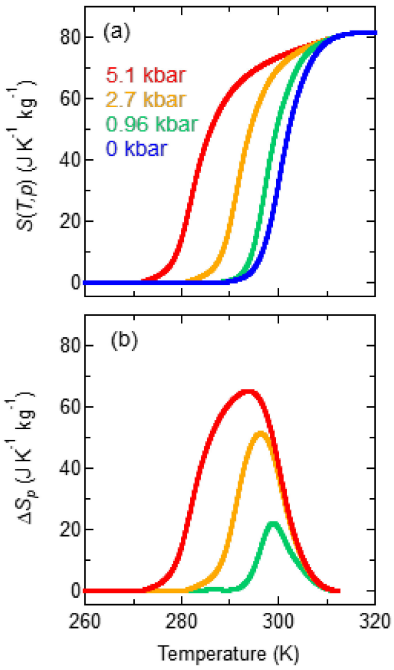

Fig. 7. (a) Entropy as functions of temperature and (b) isothermal entropy changes of $NdCu_3Fe_4O_{12}$ under various applied pressures.

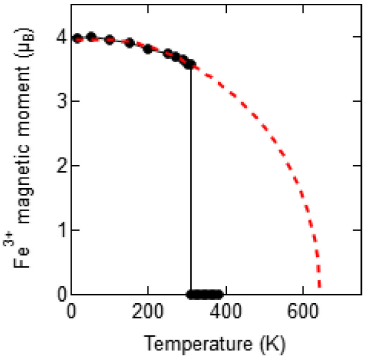

Fig. 8. Temperature dependence of the refined Fe^{3+} magnetic moment in $NdCu_3Fe_4O_{12}$. The fitting for the refined moments with an $S = 5/2$ Brillouin function is also shown in a dashed curve.

expected to be $RIn(2S + 1) = 79\,J\,K^{-1}\,kg^{-1}$. The value is more than 90 % of the observed total entropy change, and thus, most of the magnetic entropy is concluded to be responsible for the total entropy change. In normal second-order magnetic transitions the magnetic entropies are gradually changed below the magnetic transition temperatures. In the present $NdCu_3Fe_4O_{12}$, in contrast, the magnetic entropy is abruptly yielded by the unusual first-order magnetic transition induced by the intermetallic-charge-transfer transition.

Because the intermetallic-charge-transfer transition temperature of $LnCu_3Fe_4O_{12}$ is changed by the chemical substitution at the A-site,[24)–26),33)] similar fine control of the effective operating temperature for the thermal control by the caloric effect is also possible.

6. Conclusions

Novel thermo-related functional properties, negative-thermal-expansion and a caloric effect, induced by intermetallic-charge-transfer transitions in A-site-ordered quadruple perovskites $LnCu_3Fe_4O_{12}$ were highlighted. The compounds were synthesized under high-pressure conditions and contain the unusually high-valence $Fe^{3.75+}$ ions, whose electronic instabilities were relieved by the charge transitions. The negative-thermal-expansion property was well explained by the size effect of constituent ions by the charge changes. The large barocaloric effect with the significant latent heat was caused by the unusual first-order magnetic entropy change induced by the charge transition. In the compounds, charge, spin, and lattice degrees of freedom are strongly correlated, and the primarily charge transitions cause unusual changes in the crystal and electronic properties, some of which can be utilized as functional properties.

Acknowledgements The works highlighted here were done in collaboration with students, postdocs, and staff members in ICR, Kyoto University. The author gratefully acknowledges the discussion with Youwen Long, Yoshihisa Kosugi, Daisuke Kan, Masato Goto, Takashi Saito, Masaki Azuma, and Mikio Takano. The works were partly supported by many domestic and international collaboration projects, especially by Grants-in-Aid for Scientific Research (Nos. 19H05823, 20K20547, 20H00397, 22KK0075 and 23H05457), the grant for the International Collaborative Research Program of Institute for Chemical Research in Kyoto University from MEXT of Japan, and Advanced International Collaborative Research Program (AdCORP) Grant No. 0MJKB2304 by Japan Science and Technology Agency (JST).

References

1) J. B. MacChesney, R. C. Sherwood and J. F. Potter, *J. Chem. Phys.*, 43, 1907–1913 (1965).
2) M. Takano, N. Nakanishi, Y. Takeda, S. Naka and T. Takada, *Mater. Res. Bull.*, 12, 923–928 (1977).
3) Y. Takeda, S. Naka, M. Takano, T. Shinjo, T. Takada and M. Shimada, *Mater. Res. Bull.*, 13, 61–66 (1978).
4) Y. Shimakawa and M. Takano, *Z. Anorg. Allg. Chem.*, 635, 1882–1889 (2009).
5) W. T. Chen, T. Saito, N. Hayashi, M. Takano and Y. Shimakawa, *Sci. Rep.-UK*, 2, 449 (2012).
6) Y. Shimakawa, *J. Phys. D Appl. Phys.*, 48, 504006 (2015).
7) F. D. Romero and Y. Shimakawa, *Chem. Commun.*, 55, 3690–3696 (2019).
8) M. Takano, J. Kawachi, N. Nakanishi and Y. Takeda, *J. Solid State Chem.*, 39, 75–78 (1981).
9) P. D. Battle, T. C. Gibb and S. Nixon, *J. Solid State Chem.*, 77, 124–131 (1988).
10) S. Kawasaki, M. Takano and Y. Takeda, *Solid State Ionics*, 108, 221–226 (1998).
11) I. Yamada, K. Takata, N. Hayashi, S. Shinohara, M. Azuma, S. Mori, S. Muranaka, Y. Shimakawa and M. Takano, *Angew. Chem. Int. Edit.*, 47, 7032–7035 (2008).

12) Y. W. Long, N. Hayashi, T. Saito, M. Azuma, S. Muranaka and Y. Shimakawa, *Nature*, **458**, 60–63 (2009).
13) T. Takeda, R. Kanno, Y. Kawamoto, M. Takano, S. Kawasaki, T. Kamiyama and F. Izumi, *Solid State Sci.*, **2**, 673–687 (2000).
14) P. M. Woodward, D. E. Cox, E. Mosphopoulou, A. W. Sleight and S. Morimoto, *Phys. Rev. B*, **62**, 844–855 (2000).
15) T. Seda and G. R. Hearne, *J. Phys.-Condens. Mat.*, **16**, 2707–2718 (2004).
16) M. Azuma, S. Carlsson, J. Rodgers, M. G. Tucker, M. Tsujimoto, S. Ishiwata, S. Isoda, Y. Shimakawa, M. Takano and J. P. Attfield, *J. Am. Chem. Soc.*, **129**, 14433–14436 (2007).
17) X.-Y. Liu, "Modern Inorganic Synthetic Chemistry", 2nd ed., ScienceDirect (2017) pp. 105–141.
18) M. Takano, Y. Takeda and O. Ohtaka, in "Encyclopedia of Inorganic Chemistry", ed. R. B. King, John Wiley & Sons, Chichester (1994) Vol. 3, p. 1372.
19) Y. Shimakawa, *Inorg. Chem.*, **47**, 8562–8570 (2008).
20) A. N. Vasil'ev and O. S. Volkova, *Low Temp. Phys.*, **39**, 895–914 (2007).
21) P. Woodward, *Acta Crystallogr. B*, **53**, 32–43 (1997).
22) P. Woodward, *Acta Crystallogr. B*, **53**, 44–66 (1997).
23) C. J. Howard and H. T. Stokes, *Acta Crystallogr. B*, **54**, 782–789 (1998).
24) W. Long, T. Saito, T. Tohyama, K. Oka, M. Azuma and Y. Shimakawa, *Inorg. Chem.*, **48**, 8489–8492 (2009).
25) I. Yamada, H. Etani, K. Tsuchida, S. Marukawa, N. Hayashi, T. Kawakami, M. Mizumaki, K. Ohgushi, Y. Kusano, J. Kim, N. Tsuji, R. Takahashi, N. Nishiyama, T. Inoue, T. Irifune and M. Takano, *Inorg. Chem.*, **52**, 13751–13761 (2013).
26) Y. Shimakawa, M. Lufaso and P. M. Woodward, *APL Mater.*, **6**, 086106 (2018).
27) Y.-Y. Chin, H.-J. Lin, Z. Hu, Y. Shimakawa and C.-T. Chen, *Physica B*, **568**, 92–95 (2019).
28) M. Mizumaki, W.-T. Chen, T. Saito, I. Yamada, J. P. Attfield and Y. Shimakawa, *Phys. Rev. B*, **84**, 094418 (2011).
29) Y. Shimakawa and M. Mizumaki, *J. Phys.-Condens. Mat.*, **26**, 473203 (2014).
30) G. D. Barrera, J. A. O. Bruno, T. H. K. Barron and N. L. Allan, *J. Phys.-Condens. Mat.*, **17**, R217–R252 (2005).
31) M. Miller, C. W. Smith, D. S. Mackenzie and K. E. Evans, *J. Mater. Sci.*, **44**, 5441–5451 (2009).
32) M. B. Jakubinek, C. A. Whitman and M. A. White, *J. Therm. Anal. Calorim.*, **99**, 165–172 (2010).
33) M. W. Lufaso and P. M. Woodward, *Acta Crystallogr. B*, **57**, 725–738 (2001).
34) M. W. Lufaso, P. W. Barnes and P. M. Woodward, *Acta Crystallogr. B*, **62**, 397–410 (2006).
35) I. D. Brown, A. Dabkowski and A. McCleary, *Acta Crystallogr. B*, **53**, 750–761 (1997).
36) R. Shannon, *Acta Crystallogr. A*, **32**, 751–767 (1976).
37) Y. Kosugi, M. Goto, Z. Tan, A. Fujita, T. Saito, T. Kamiyama, W. T. Chen, Y. C. Chuang, H. S. Sheu, D. Kan and Y. Shimakawa, *Adv. Funct. Mater.*, **31**, 2009476 (2021).
38) A. Gschneidner, V. K. Pecharsky and A. O. Tsokol, *Rep. Prog. Phys.*, **68**, 1479–1539 (2005).
39) M. Valant, *Prog. Mater. Sci.*, **57**, 980–1009 (2012).
40) S. Fähler, U. K. Rößler, O. Kastner, J. Eckert, G. Eggeler, H. Emmerich, P. Entel, S. Müller, E. Quandt and K. Albe, *Energy Technol.*, **14**, 10–19 (2012).
41) X. Moya, S. Kar-Narayan and N. D. Mathur, *Nat. Mater.*, **13**, 439–450 (2014).
42) L. Mañosa and A. Planes, *Adv. Mater.*, **29**, 1603607 (2017).
43) A. S. Mischenko, Q. Zhang, J. F. Scott, R. W. Whatmore and N. D. Mathur, *Science*, **311**, 1270–1271 (2006).
44) B. Neese, B. Chu, S. G. Lu, Y. Wang, E. Furman and Q. M. Zhang, *Science*, **321**, 821–823 (2008).
45) D. Matsunami and A. Fujita, *Appl. Phys. Lett.*, **106**, 042901 (2015).
46) L. Mañosa, D. González-Alonso, A. Planes, E. Bonnot, M. Barrio, J. L. Tamarit, S. Aksoy and M. Acet, *Nat. Mater.*, **9**, 478–481 (2010).
47) D. Matsunami, A. Fujita, K. Takenaka and M. Kano, *Nat. Mater.*, **14**, 73–78 (2015).
48) Y. Shimakawa and Y. Kosugi, *J. Mater. Chem. A*, Advanced Article (2023).
49) T. Samanta, P. Lloveras, A. U. Saleheen, D. L. Lepkowski, E. Kramer, I. Dubenko, P. W. Adams, D. P. Young, M. Barrio, J. L. Tamarit, N. Ali and S. Stadler, *Appl. Phys. Lett.*, **112**, 021907 (2018).
50) W. T. Chen, Y. Long, T. Saito, J. P. Attfield and Y. Shimakawa, *J. Mater. Chem.*, **20**, 7282–7286 (2010).
51) Y. Kosugi, M. Goto, Z. Tan, D. Kan, M. Isobe, K. Yoshii, M. Mizumaki, A. Fujita, H. Takagi and Y. Shimakawa, *Sci. Rep.-UK*, **11**, 12682 (2021).

Yuichi Shimakawa is a professor in Institute of Chemical Research, Kyoto University. He received his Ph.D. from Kyoto University in 1993. He was a Principal Researcher in Fundamental Research Laboratories, NEC Corporation, and then joined Kyoto University as a Professor in 2003. His research interests are in the solid-state chemistry and materials science of transition metal oxides, which have interesting and useful properties. The research focuses on the search for new oxide materials with novel functional properties. He is a Fellow of the Royal Society of Chemistry, UK.